Na-Induced Correlations in Na_xCoO_2

C. A. Marianetti[1] and G. Kotliar[1,2,3]

[1]*Department of Physics and Astronomy and Center for Condensed Matter Theory, Rutgers University,
Piscataway, New Jersey 08854-8019, USA*
[2]*Service de Physique Theorique, CEA Saclay, 91191 Gif-sur-Yvette, France*
[3]*Centre de Physique Theorique, Ecole Polytechnique, 91128 Palaiseau Cedex, France*
(Received 8 May 2006; published 26 April 2007)

Increasing experimental evidence is building which indicates that signatures of strong correlations are present in the Na-rich region of Na_xCoO_2 (i.e., $x \approx 0.7$) and absent in the Na-poor region (i.e., $x \approx 0.3$). This is unexpected, given that $NaCoO_2$ is a band insulator and CoO_2 has an integer-filled open shell, making it a candidate for strong correlations. We explain these experimental observations by presenting a minimal low-energy Hamiltonian for the cobaltates and solving it using density functional theory and dynamical mean-field theory. The Na potential is shown to be a key element in understanding correlations in this material. Furthermore, density functional theory calculations for the realistic Na ordering predict a *binary* perturbation of the Co sites which correlates with the Na_1 sites (i.e., Na sites above or below Co sites).

PACS numbers: 71.27.+a

The qualitative features of the cobaltate phase diagram have been experimentally established [1]. Fermi-liquid-type behavior is observed in the Na-poor region, while strongly correlated behavior is observed in the Na-rich region. For example, magnetic susceptibility measurements show Pauli-like behavior for $x \approx 0.3$ and Curie-Weiss behavior for $x \approx 0.7$ [1] (for further references, see [2,3]).

These observations are counterintuitive, given our conventional understanding of Na_xCoO_2. In $NaCoO_2$, Co is in the 3+ configuration and thus has six electrons. The cubic component of the crystal field splits the d manifold into a set of threefold t_{2g} orbitals and twofold e_g orbitals, while the trigonal component will further split the t_{2g} orbitals into a_{1g} and e'_g. In this scenario, the six electrons of the Co will fill the t_{2g} orbitals (i.e., $a_{1g} + e'_g$), resulting in a band insulator [4,5]. On the contrary, in CoO_2, the Co will be in a 4+ configuration having 5 electrons in the t_{2g} shell and may be either a metal or a Mott insulator.

There are two main puzzles posed by the above listed experimental observations. First, given that $NaCoO_2$ is a band insulator, it is difficult to understand why correlations are observed for the nearby composition of $x = 0.7$. The density of holes will be relatively low, and, therefore, the on-site Coulomb repulsion will have a minimal effect. Second, one would expect correlations to increase as the system is doped towards $x = 0.3$ as the hole density in the t_{2g} shell is increasing towards integer occupancy with an open shell. We resolve this puzzle by proposing a minimal low-energy Hamiltonian which captures the essential physics and solve it within dynamical mean-field theory (DMFT):

$$H = \sum_{ij\alpha\beta\sigma} t_{\alpha\beta} c^+_{i\alpha\sigma} c_{j\beta\sigma} + \sum_{i\alpha\beta\sigma\sigma'} U^{\sigma\sigma'}_{\alpha\beta} n_{i\alpha\sigma} n_{i\beta\sigma'} + \sum_{i\alpha\sigma} \epsilon_{\alpha i} n_{\alpha i\sigma},$$

(1)

where i, j are site indices, α, β are orbital indices running over a_{1g} and e'_g, t is the hopping parameter, U is the on-site Coulomb repulsions, and ϵ is the on-site potential which mimics the Na potential. It should be emphasized that the orbitals to which the creation operators refer are low-energy orbitals, effectively composed of oxygen p orbitals as well as Co d orbitals which compose the t_{2g} antibonding manifold. All of the parameters of the Hamiltonian are, in general, functions of the total density, as the system rehybridizes [6] as a function of doping.

The parameters of the Hamiltonian are obtained using local-density approximation (LDA) calculations on $NaCoO_2$ and CoO_2 to be used for DMFT calculations in the Na-rich and the Na-poor region, respectively. The projected density of states (DOS) for the a_{1g} and e'_g states is shown in Fig. 2. In both cases, the a_{1g} orbital has the overwhelming fraction of hole density. The doping dependence of the hopping parameters is substantial, given the changes in the shape of the DOS and given that the total bandwidth increases by 0.25 eV for CoO_2. Detailed cluster calculations for $LiCoO_2$ fit the on-site U to the experimental photoemission yielding $U = 3.5$ eV [7]. This should be very similar to $NaCoO_2$, and we use a slightly reduced value of $U = 3$ eV because we are considering low-energy orbitals. Additionally, we assume U to be independent of doping. A nearest-neighbor Coulomb interaction should be added to Eq. (1) in order to assist in forming charge-ordered phases [8], and, in single-site DMFT, this results in a Hartree shift.

The on-site potential ϵ is treated as a *random binary* variable, and the fact that it is binary will be justified in the LDA calculations below. Treating the potential as random should be accurate for average quantities in the Na-ordered phases or even k-resolved quantities in the disordered region of the phase diagram. A fraction x_1 of the lattice sites will have an on-site potential ϵ_1, while $(1 - x_1)$ sites

will have an on-site potential $\epsilon_2 = x_1\epsilon_1/(x_1 - 1)$. We will assume that x_{ϵ_1} corresponds to $1 - x_{Na}$, where x_{Na} is the fraction of Na in the material. This also will be justified by our LDA calculations.

We propose that the Na potential plays a critical role in the behavior of this material. In a previous study of Li_xCoO_2 [9] (a very similar material), LDA calculations demonstrated that, in the dilute Li-vacancy region of the phase diagram, the Li vacancy binds the hole which is usually doped into the t_{2g} band and, hence, forms a half-filled impurity band split off from the valence band (analogous to phosphorous-doped silicon, except the vacancies are highly mobile). Because of the fact that the impurity band is half-filled, it may be strongly correlated and form a Mott insulator if the on-site interaction is sufficiently strong. This behavior persists until enough holes are present to screen the Li vacancies upon which the more standard picture of doping into the t_{2g} states is recovered. The LDA calculations predict the impurity band to completely merge into the valence band once $x \approx 0.98$. Because of the similarities of the two materials, it is likely that a similar scenario occurs in Na_xCoO_2. Of course, the experiments of interest are in a region of much higher doping (i.e., $x \approx 0.7$), where it is implausible that an impurity band would persist. However, it is likely that the Na vacancies will still act as a strong perturbation towards the Co sites. Therefore, it is possible that the Na vacancy potential will cause certain Co sites to be higher in energy and possess a higher occupation than the average number of holes. Increasing the occupation of a given site towards integer filling will favor moment formation, assuming that the on-site Coulomb repulsion is sufficiently strong. This phenomenon has been studied in detail in the context of model Hubbard Hamiltonians [10]. Merino *et al.* suggested a Hubbard model on a triangular lattice in the presence of an ordered potential in order to explain the correlated behavior observed in Na_xCoO_2 [11]. They note that, in the limit of strong coupling of the ordered potential, correlations will be formed, similar to our work. NMR measurements strongly support this notion of certain Co sites being favored, as there are distinct Co sites for $x = 0.7$ while there are not for $x = 0.3$ [12]. The fact that only one site is observed at $x = 0.3$ supports the notion that the Na potential is well screened and no longer a significant perturbation for small x.

In order to understand the effect of the Na potential described by the on-site potential ϵ in Eq. (1), we performed LDA calculations on the $x = \frac{1}{3}$ and $x = \frac{3}{4}$ unit cells which were experimentally determined by Zandbergen *et al.* [13]. These unit cells have 6 and 16 formula units for the $x = \frac{1}{3}$ and $x = \frac{3}{4}$ unit cells, respectively, and both contain equal numbers of occupied Na_1 and Na_2 sites. The Na_1 sites project directly onto the triangular Co lattice, while the Na_2 sites project onto the centroids of the Co triangular lattice [13]. All LDA calculations were per-

formed using the Vienna *ab initio* simulation code (VASP) [14]. In order to quantify the effect of the Na potential on the different orbitals, the first moment $m_{i\alpha}$ of the projected DOS (i.e., the on-site orbital energy) of the oxygen and cobalt orbitals is calculated for each site of the supercell. $m_{i\alpha} = \int \rho_{i\alpha}(\epsilon)\epsilon d\epsilon / \int \rho_{i\alpha}(\epsilon)d\epsilon$, where the indices i and α are the site and orbital indices, respectively. The deviation of the orbital energy from the site average is shown in Fig. 1 (i.e., $m_{i\alpha} - \bar{m}_\alpha$). Remarkably, the results are roughly binary distributions as evidenced by the horizontal lines which are formed by the data points. The Na ordering causes each site to be perturbed, resulting in either a high- or low-energy orbital on a given site. The oxygen orbitals are perturbed the most, followed by the a_{1g} and e'_g orbitals. The perturbations are substantially smaller for $x = \frac{1}{3}$ as compared to $x = \frac{3}{4}$, which is expected, given that a larger amount of hole density is present at $x = \frac{1}{3}$ to screen the Na potential. A very simple rule governs the observed behavior. In the $x = \frac{3}{4}$ structure, all of the low-energy a_{1g} and e'_g orbitals have one nearest-neighbor Na_1 present, while the high-energy orbitals do not. There are 6 Na_1 sites occupied in this unit cell, each of which will have 2 Co nearest neighbors, and, hence, there are 4 high-energy Co sites and 12 low-energy sites. For the $x = \frac{1}{3}$ structure, the a_{1g} orbital follows the same rule. However, the e'_g orbitals are perturbed in the opposite direction in this case. However, the perturbations of the e'_g orbitals are all less than 2 meV and should be considered carefully. The splitting of the oxygen orbitals also follows a simple rule in the $x = \frac{3}{4}$ structure. All of the low-energy oxygens have three nearest-neighbor Na, while the high-energy oxygens only have two nearest-neighbor Na. For the $x = \frac{1}{3}$ struc-
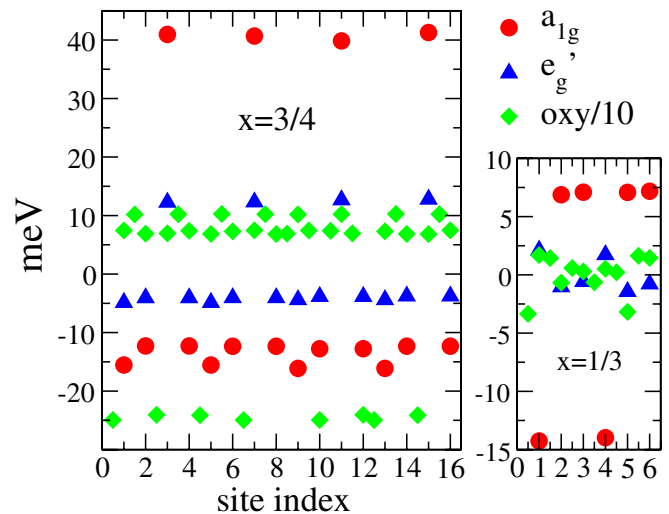

FIG. 1 (color online).   The on-site orbital energy $m_{i\alpha}$ relative to the average for various orbitals at each site in the unit cell. The energies for the oxygen orbitals have been divided by 10. The left and right panels correspond to $Na_{3/4}CoO_2$ and $Na_{1/3}CoO_2$, respectively.

ture, the oxygen does not split into a binary distribution, but it can be roughly understood as a ternary distribution if one analyzes both nearest- and next-nearest-neighbor Na. The low-energy oxygen have three neighboring Na, and the high-energy oxygens have two Na_1 neighbors, while the intermediate-energy oxygens have two Na_2 neighbors. Regardless, the a_{1g} and e'_g orbitals seem to depend only on the positions of the Na_1. This seems very reasonable for the a_{1g} orbitals, given that they point directly towards the Na_1 sites (i.e., $a_{1g} = d_{z^2}$ in the hexagonal coordinate system). This can be very important for several aspects of the low-energy behavior in this material. For example, this effect would tend to drive charge ordering to occur on the Co sites which are located directly above or below the occupied Na_1 sites. Additionally, this could effect the stabilization the pockets in the Fermi surface as the two orbitals are perturbed differently. For a recent study on the effect of Na on the Fermi surface, see [15].

Obtaining parameters for a model Hamiltonian from LDA calculations is still an open problem. Therefore, we simply extract the qualitative effects of the Na potential. The binary splitting of the oxygen for $x = \frac{3}{4}$ is roughly 350 meV, while for $x = \frac{1}{3}$ the maximum splitting is roughly 50 meV. This should be relevant to the low-energy Hamiltonian, given that the hole density on the t_{2g} states has associated hole density on the oxygen via the rehybridization mechanism [6]. The changes on the Co are smaller, with the a_{1g} splitting being roughly 55 and 20 meV for $x = \frac{3}{4}$ and $x = \frac{1}{3}$, respectively. This is to be expected, given that these states are near the Fermi energy and are not only well screened but overscreened by LDA, and, thus, their bare values may be significantly larger. We take a value of $\epsilon_i = 400$ meV for $x = \frac{3}{4}$ and $\epsilon_1 = \frac{400}{3}$ meV for $x = \frac{1}{3}$, reflecting the fact that $x = \frac{1}{3}$ is more screened. A more appropriate value for $x = \frac{1}{3}$ might be $\epsilon_1 = 0$, given that only a single Co is observed in NMR [12], and we explore this as well. We conservatively assume ϵ to be orbitally independent, which will make it more difficult to form correlations near the band insulator. Below, we will demonstrate that these estimates yield predictions consistent with experimental observations.

With these order-of-magnitude estimates, we shall now proceed to solve the proposed Hamiltonian [Eq. (1)] within DMFT [16,17], including the additional effect of binary disorder (see [17] for references). In this case, there will be two impurity models, which represent the two different binary environments. We begin with a guess for the average hybridization function Δ and then construct the bath function $G_0 = (i\omega_n - E_{imp} + \mu - \Delta)^{-1}$, where E_{imp} is the average impurity level and μ is the chemical potential. We then construct the two disorder bath functions $G_0^{\epsilon_1} = (G_0^{-1} - \epsilon_1)^{-1}$ and $G_0^{\epsilon_2} = (G_0^{-1} - \epsilon_2)^{-1}$. The two corresponding impurity problems are then solved, and the average Greens function is constructed as $G = x_{\epsilon_1} G_{\epsilon_1} +$

$(1 - x_{\epsilon_1}) G_{\epsilon_2}$. The average self-energy is then constructed using Dyson's equation $\Sigma(i\omega_n) = G_0^{-1}(i\omega_n) - G^{-1}(i\omega_n)$. Finally, the DMFT self-consistency condition is performed:

$$G_0(i\omega_n) = \left[\Sigma(i\omega_n) + \left(\sum_k \frac{1}{i\omega_n - H_k + \mu - \Sigma(i\omega_n)} \right)^{-1} \right]^{-1},$$

(2)

where H_k is the homogeneous Hamiltonian [i.e., Eq. (1) with $\epsilon = 0$] in k space. The entire process is then repeated until convergence is achieved. Given that the local Green's function is diagonal (i.e., $a_{1g} + e'_g$), the summation over k in Eq. (2) can be approximated by a Hilbert transform (see [17]).

The DMFT impurity problem is solved using the continuous time quantum Monte Carlo (CTQMC) method (see [18,19]) using the DMFTLAB code [20]. We begin by considering the Na-rich case of $x = 0.7$. The spectral functions for the a_{1g} orbital clearly shows the correlations increasing as the on-site potential is increased (Fig. 2). The states at the Fermi energy are suppressed, and spectral weight is transferred from low energies to higher energies as the on-site potential is increased. Another useful quantity to analyze is the local magnetic susceptibility (see Fig. 3), which is one of the key experimental measurements. The susceptibility is relatively flat for the case with zero on-site potential, while a Curie-Weiss tail is clearly formed for the case when an on-site potential of 0.4 eV is included. In that latter case, 30% of the sites have 0.73 holes, while 70% of the sites have 0.1 holes. This is qualitatively similar to what is observed in NMR experiments [12]. Thus, the ϵ_1 site becomes the favored site, receiving significantly more hole density and being driven towards integer filling where a local moment forms.
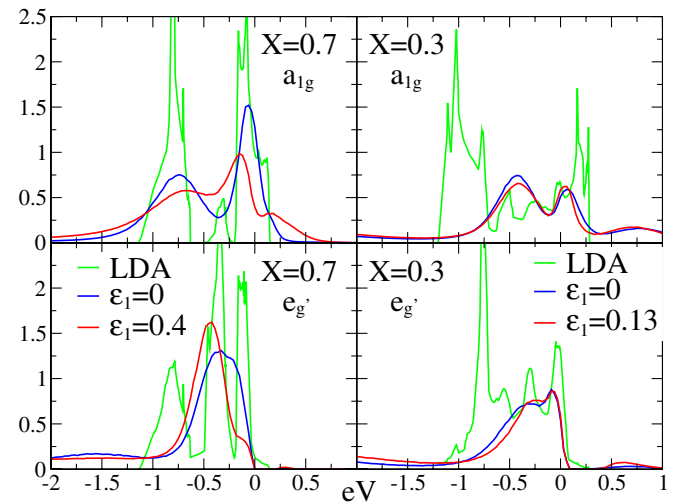

FIG. 2 (color online).   Spectral functions for Na_xCoO_2 at $T = 290$ K.
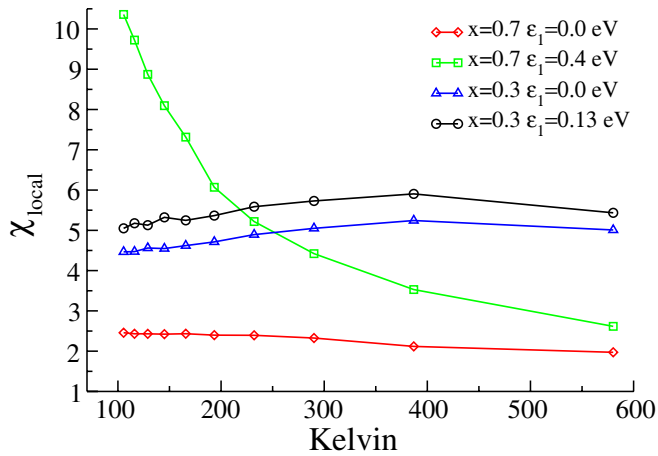
FIG. 3 (color online). Local magnetic susceptibility versus temperature for Na_xCoO_2.

Now we proceed to the Na-poor region and perform calculations at $x = \frac{1}{3}$. The spectral function for the a_{1g} orbital shows some indication of correlations as some spectral weight has been transferred to higher energies (see Fig. 2). Additionally, the e'_g orbitals show a small occupation in this case (see [21] for a detailed discussion of e'_g pockets). The on-site potential has only a small effect on the spectral function. The main result is that the magnetic susceptibilities shows only a weak temperature dependence in both cases, and there is no sign of a Curie-Weiss tail (see Fig. 3). The on-site potential clearly enhances the susceptibility but is not capable of building strong correlations. The on-site potential creates two distinct sites with 70% having 0.76 holes and 30% having 0.5 holes. Both susceptibilities cross the Curie tail of the $x = 0.7$ case in the vicinity of room temperature, similar to the crossover observed in experiment between 150–250 K [1].

Because of the computational demands of CTQMC, our calculations are currently limited to temperatures above 100 K, so we cannot predict the fate of the local moments in $Na_{0.7}CoO_2$ at lower temperatures. However, our model should be applicable at zero temperature. Our model clearly predicts the formation of local moments in $Na_{0.7}CoO_2$ for $T > 100$ K, as observed in experiment [1], and there are a few possible outcomes for the behavior of the moments at low temperatures. The local moments may be screened, resulting in a very heavy normal Fermi liquid. Alternatively, the magnetic moments may order ferromagnetically, antiferromagnetically, or at some other wave vector. Experiments predict a magnetic phase transition for $x = 0.75$ at $T = 22$ K [22], and neutron diffraction measurements [23] are interpreted as showing ferromagnetism within the Co planes. These observations may serve as future tests of our model, assuming these low temperatures may be directly reached or that the vertex function may be calculated at sufficiently low temperatures.

In conclusion, we have proposed a low-energy Hamiltonian that is capable of explaining the observation of correlations near a band insulator in the Na-rich region of the doped cobaltates. Realistic parameters for the Hamiltonian estimated from LDA calculations reproduce the generic behavior observed in the experimental magnetic susceptibility measurements. The Na potential is shown to be a key element in forming correlations near the band insulator. LDA calculations for the experimentally predicted Na orderings imply that the Na_1 sites act as a binary perturbing potential of the Co sites. Our model may be further improved by treating spatial correlation of the on-site potential, improved downfolding techniques to obtain the parameters of the low-energy Hamiltonian, inclusion of polarons, and the inclusion of the e_g states. The e_g states are needed to describe the high-energy behavior of this system and, additionally, may cause further renormalization at low energies. Including these effects may allow for smaller values of the on-site potential ϵ in order to achieve the same qualitative effects.

[1] M. L. Foo *et al.*, Phys. Rev. Lett. **92**, 247001 (2004).
[2] F. C. Chou, J. H. Cho, and Y. S. Lee, Phys. Rev. B **70**, 144526 (2004).
[3] Y. Ihara *et al.*, J. Phys. Soc. Jpn. **73**, 2963 (2004).
[4] C. D. Vaulx *et al.*, Phys. Rev. Lett. **95**, 186405 (2005).
[5] G. Lang *et al.*, Phys. Rev. B **72**, 094404 (2005).
[6] C. A. Marianetti, G. Kotliar, and G. Ceder, Phys. Rev. Lett. **92**, 196405 (2004).
[7] J. Vanelp *et al.*, Phys. Rev. B **44**, 6090 (1991).
[8] O. I. Motrunich and P. A. Lee, Phys. Rev. B **69**, 214516 (2004).
[9] C. A. Marianetti, G. Kotliar, and G. Ceder, Nat. Mater. **3**, 627 (2004).
[10] K. Byczuk, M. Ulmke, and D. Vollhardt, Phys. Rev. Lett. **90**, 196403 (2003).
[11] J. Merino, B. J. Powell, and R. H. Mckenzie, cond-mat/ 0512696.
[12] I. R. Mukhamedshin *et al.*, Phys. Rev. Lett. **94**, 247602 (2005).
[13] H. W. Zandbergen *et al.*, Phys. Rev. B **70**, 024101 (2004).
[14] G. Kresse and J. Furthmuller, Phys. Rev. B **54**, 11 169 (1996).
[15] D. J. Singh and D. Kasinathan, cond-mat/0604002.
[16] G. Kotliar *et al.*, Rev. Mod. Phys. **78**, 865 (2006).
[17] A. Georges *et al.*, Rev. Mod. Phys. **68**, 13 (1996).
[18] P. Werner and A. J. Millis, cond-mat/0607136.
[19] K. Haule, cond-mat/0612172.
[20] O. Parcollet and C. A. Marianetti, http://dmft.rutgers.edu.
[21] C. A. Marianetti, K. Haule, and O. Parcollet, cond-mat/ 0612606.
[22] T. Motohashi *et al.*, Physica (Amsterdam) **329B**, 914 (2003).
[23] A. T. Boothroyd *et al.*, Phys. Rev. Lett. **92**, 197201 (2004).